

REPORT SM-6  
November 1965

INITIAL POST-BUCKLING BEHAVIOR OF TOROIDAL SHELL SEGMENTS\*

John W. Hutchinson\*\*

Harvard University, Cambridge, Massachusetts

*Handwritten:* N66-18314  
MK 2.00  
30

ABSTRACT

The initial post-buckling behavior of double curvature shell segments subject to several loading conditions is determined on the basis of Koiter's general theory of initial post-buckling behavior. Previously, the classical buckling loads associated with these shells were shown to be strongly dependent on the two radii of curvature and their relative magnitudes. Here, the initial post-buckling behavior and associated imperfection-sensitivity are also seen to be strongly dependent on the two curvatures.

*Handwritten:* Author

INTRODUCTION

Among those structures whose buckling strengths are known to be highly sensitive to structural imperfections are spherical and cylindrical shells subject to external pressure, axially loaded narrow cylindrical panels, some simple trusses and, of course, the axially compressed cylindrical shell. The classical (linear) buckling analysis of such a structure, by itself, is incapable of predicting the buckling strength. Accurate predictions for a given structure require exact knowledge of the initial imperfections of the unloaded structure; but, in general, such information is not at the disposal of either the analyst or designer. To

\* This work was supported in part by the National Aeronautics and Space Administration under Grant NsG-559, and by the Division of Engineering and Applied Physics, Harvard University.

\*\* Assistant Professor of Structural Mechanics.

N66-18314

(ACCESSION NUMBER)	(THRU)
37	1
(PAGES)	(CODE)
CR-66057	32
(NASA CR OR TMX OR AD NUMBER)	(CATEGORY)

FACILITY FORM 602

Distribution of this report is provided i information exchange. Responsibility resides in the author or organization ti

date, mainly because of the difficulty of measuring imperfections of actual as well as test specimens, analytic work has served to provide information as to the relative imperfection-sensitivity of structures and, thus, to qualitatively establish the validity or non-validity of the classical buckling analysis.

In this paper some double curvature shell structures, whose classical buckling behavior has only recently been studied, are investigated with the view toward determining their initial post-buckling behavior and, what is closely related, the dependence of their buckling strengths on imperfections in the form of initial deviations of the shell middle surface from the perfect configuration. This study is made within the framework of Koiter's general theory of initial post-buckling behavior [1].

The shell segments shown in Figure 1 can be thought of as sections of complete toroidal shells. The classical buckling analysis of these shells has been given by Stein and McElman [2] for three different pressure loadings. Results of their analysis for the case of buckling under lateral pressure are reproduced in Figure 2. Here, the buckling parameter,  $K = pr_y \ell^2 / \pi^2 D$  (where  $p$  is the lateral pressure,  $D = Eh^3/12(1-\nu^2)$  is the bending stiffness,  $h$  is the shell thickness and  $\nu$  is Poisson's ratio) is a function of the length parameter

$$z = \sqrt{(1-\nu^2)} \ell^2 / r_y h$$

and the ratio of the two radii of curvatures  $r_y/r_x$ . An elucidation of further details relevant to this plot, such as boundary conditions, will be given in the next section. At this point, however, attention is drawn to the significant difference between the predicted buckling strengths of the bowed-out and the bowed-in shells which are otherwise of essentially the same dimensions. On the basis of the classical buckling analysis the buckling strength of the bowed-out shell can be several orders of magnitude larger than that of the bowed-in configuration. One

might conjecture, and, indeed, this will prove to be the case, that the initial post-buckling analysis indicates a significantly increased imperfection-sensitivity hand-in-hand with the higher classical buckling strength.

Two other loading conditions are studied in addition to the lateral pressure case. Quite similar, yet more imperfection-sensitive, is the external pressure case. In the third case the classical and initial post-buckling behavior of the bowed-out segments subject to axial tension is determined.

### CLASSICAL BUCKLING ANALYSIS

Here a brief exposition of Stein and McElman's classical analysis is given. Buckling under axial tension, although not considered by these authors, is also included in the results given below. Donnell-type nonlinear shell theory is employed in the classical, as well as the initial post-buckling, analysis of the toroidal segments. Consideration is restricted to segments which are shallow with respect to the axial coordinate, that is  $l/r_x \ll 1$ . The linear Donnell buckling equations, given by Stein and McElman, are written here in terms of the normal displacement  $w$  and a stress function  $f$

$$D\nabla^4 w + \frac{1}{r_y} f_{,xx} + \frac{1}{r_x} f_{,yy} - \lambda N_x^0 w_{,xx} - \lambda N_y^0 w_{,yy} = 0 \quad (1)$$

and

$$\frac{1}{Eh} \nabla^4 f - \frac{1}{r_y} w_{,xx} - \frac{1}{r_x} w_{,yy} = 0 \quad (2)$$

where  $E$  is Young's Modulus and the assumption of shallowness in the axial direction permits us to write  $\nabla^4 = (f_{,xx} + f_{,yy})^2$ . The additional buckling membrane stresses are given by  $N_x = f_{,yy}$ ,  $N_y = f_{,xx}$  and  $N_{xy} = -f_{,xy}$ .

In Equation (1)  $\lambda N_x^0$  and  $\lambda N_y^0$  represent the  $x$  and  $y$  components of the resultant membrane stresses associated with the prebuckling deformation of the perfect shell. Except for a narrow region near each end of the shell the

prebuckling state of stress is homogeneous and, for each loading system investigated here, is linearly dependent on the externally applied load. In this paper the edge distortions are neglected and, thus, the membrane stresses  $\lambda N_x^0$  and  $\lambda N_y^0$  are constant over the entire shell. The load parameter  $\lambda$  is linearly related to the applied load and  $N_x^0$  and  $N_y^0$  are assumed to be fixed in some definite manner depending on the particular loading system. Refined analyses for cylindrical shells [3] accounting for the end distortions have shown that, except for very short shells, the local end effects can be neglected when the buckle pattern has only one half wavelength over the axial length. It is expected that approximate calculations neglecting the edge zone distortions should not introduce significant errors as long as  $z > 10$  say. Since the underlying aim of this study is to discover the role of the two radii of curvature,  $r_x$  and  $r_y$ , in determining the initial post-buckling behavior, we follow Stein and McElman and choose the boundary conditions which are most tractable from the point of view of the analysis. At each end of the shell the normal and circumferential tangential displacements are required to vanish as is the additional buckling stress  $N_x = f_{,yy}$  and the additional bending stress  $M_x$ . In terms of  $w$  and  $f$  these are equivalent to

$$w = w_{,xx} = f_{,xx} = f = 0 \quad \text{at } x = 0, \ell \quad (3)$$

Other boundary conditions, completely clamped for example, can be expected to give quite different predictions for the classical buckling load. Nevertheless, it is felt that a complete study based on these boundary conditions should lend at least qualitative insight to the imperfection-sensitivity of similar shells with other edge conditions.

Equations (1) and (2) with the boundary conditions (3) comprise the linear eigenvalue problem for determining the classical buckling load. The eigenfunction

$$w_{mn} = \sin \frac{m\pi x}{l} \sin \frac{ny}{r_y}$$

$$f_{mn} = - \frac{Eh l^2}{\pi^2 r_y} \left[ \frac{m^2 + \bar{n}^2 r_y / r_x}{(m^2 + \bar{n}^2)^2} \right] \sin \frac{m\pi x}{l} \sin \frac{ny}{r_y}$$

is associated with the eigenvalue

$$\lambda_{mn} = - \frac{D\pi^2}{l^2} \frac{1}{(N_x^0 m^2 + N_y^0 \bar{n}^2)} \left[ (m^2 + \bar{n}^2)^2 + \frac{12z^2}{\pi^4} \frac{(m^2 + \bar{n}^2 r_y / r_x)^2}{(m^2 + \bar{n}^2)^2} \right]$$

where  $\bar{n} = n l / \pi r_y$ . The classical buckling load  $\lambda_c$  corresponds to the minimum value of  $\lambda_{mn}$  among all possible integer values of  $m$  and  $n$ . For each of the three loading conditions considered in this paper the minimum value of  $\lambda_{mn}$  always occurs for  $m = 1$ . The minimum with respect to  $n$  is found by treating  $\bar{n}$  as a continuous variable under the assumption, to be verified a posteriori, that  $n$  is sufficiently large. The restriction to  $n > 5$ , say, is necessary in any case since Donnell-type equations are being used.

The indicated calculations were carried out with the aid of a digital computer and will be presented in sections to follow. For the two pressure loadings the results are in agreement with Stein and McElman's calculations.

#### DESCRIPTION OF INITIAL POST-BUCKLING ANALYSIS

The linear buckling analysis predicts the critical load and associated buckling mode, or modes, of the structure. A unique buckling mode is predicted in every case considered in this paper. The initial post-buckling analysis of such a structure provides a single nonlinear, algebraic equation of equilibrium relating the applied load to the deflection in the buckling mode. The magnitude of the initial imperfection also appears in this equation.

The normal displacement of the buckling mode deflection is

$$w = \xi h \sin(\pi x / l) \sin(ny / r_y) \tag{4}$$

where  $n$  is determined by the classical analysis and  $\xi$  is the mode deflection relative to the shell thickness  $h$ . Initial imperfections in the form of the buckling modes are most critical if, indeed, imperfections play any degrading role at all. In the present analysis the initial deviation of the shells from the perfect toroidal form is denoted by  $\bar{w}$  and is taken to be

$$\bar{w} = \bar{\xi} h \sin(\pi x/l) \sin(ny/r_y) \quad (5)$$

where here also, the imperfection  $\bar{\xi}$  is measured relative to the shell thickness.

The equilibrium equation obtained from the Koiter analysis, valid in the initial post-buckling regime, is of the form

$$\left(1 - \frac{\lambda}{\lambda_c}\right)\xi + a\xi^2 + b\xi^3 + \dots = \frac{\lambda}{\lambda_c} \bar{\xi} + \text{order } \xi\bar{\xi} + \dots \quad (6)$$

where  $\lambda/\lambda_c$  is the ratio of the applied load  $\lambda$  to the classical buckling load  $\lambda_c$ . The derivation of this equation and the calculation of the coefficients  $a$  and  $b$  are given in the Appendix.

Each of the structure-load combinations considered in this paper is of the "cubic type"; that is,  $a$  is identically zero and the initial post-buckling behavior is determined by the term  $b\xi^3$  in the equilibrium equation. Thus the governing equation is

$$\left(1 - \frac{\lambda}{\lambda_c}\right)\xi + b\xi^3 = \frac{\lambda}{\lambda_c} \bar{\xi} \quad (7)$$

This equation is asymptotically valid for small  $\xi$  and  $\bar{\xi}$ .

The load-deflection behavior of the cubic structure is depicted in the two plots of Figure 3. The perfect structure,  $\bar{\xi} = 0$ , suffers no deflection in the  $\xi$  mode prior to buckling. At  $\lambda = \lambda_c$  bifurcation from the prebuckling state occurs. If  $b > 0$  the applied load  $\lambda$  increases with increasing deflection  $\xi$ ; while if  $b < 0$  the equilibrium curve of  $\lambda$  vs.  $\xi$  falls in the initial post-buckling region. The effect of an initial imperfection on the load-deflection

behavior is also shown in these two plots. Only in the latter case, namely  $b < 0$ , is the cubic structure imperfection-sensitive in the sense that imperfections result in reduced values of the maximum load the structure can support. An expression relating the buckling load (maximum load)  $\lambda^*$  of the imperfect structure to the imperfection magnitude for the case  $b < 0$  is easily found from Equation (7) in conjunction with the condition  $\frac{d\lambda}{d\bar{\xi}} = 0$ . This is

$$\left(1 - \frac{\lambda^*}{\lambda_c}\right)^{3/2} = \frac{3\sqrt{3}}{2} \sqrt{-b} |\bar{\xi}| \frac{\lambda^*}{\lambda_c}$$

The plot of  $\lambda^*/\lambda_c$  vs.  $\sqrt{-b} |\bar{\xi}|$  is given in Figure 4. If  $\sqrt{-b}$  is of order unity, imperfections which are small relative to the shell thickness (i.e.,  $\bar{\xi}$  a small fraction of unity) will result in large reductions of the buckling load.

The results of the  $b$  calculation for the three loading cases are presented and discussed in the next three sections; and as we have mentioned, the details of the calculations are left for the Appendix.

#### TOROIDAL SEGMENT SUBJECT TO LATERAL PRESSURE

The prebuckling state of stress of a perfect, shallow toroidal segment subject to lateral pressure  $p$  is uniform, except in a narrow region near the ends of the shell, and is given by

$$\lambda_{x}^0 = 0 \quad \text{and} \quad \lambda_{y}^0 = -pr_y \quad (8)$$

Results from the classical buckling analysis have been referred to in the introduction and are shown in Figure 2. This is a plot of the buckling parameter  $K = pr_y \ell^2 / \pi^2 D$  as a function of  $z = (1-\nu^2)^{1/2} \ell^2 / r_y h$  for several values of  $r_y / r_x$ .

Figure 5 contains plots of  $b/(1-\nu^2)$ , again, as a function of  $z$  for several values of  $r_y / r_x$ . The bowed-out segments,  $r_y / r_x > 0$ , are imperfection-sensitive (i.e.,  $b < 0$ ) over a major part of the range of  $z$ . The more the toroidal shell

is bowed-out the more negative is  $b$  and, thus, the more sensitive the structure to imperfections. There is a significant range, even for the cylindrical shell ( $r_y/r_x = 0$ ), for which  $\sqrt{-b}$  is of order unity, and small imperfections relative to the shell thickness will, therefore, result in significant reductions in the buckling pressure. For configurations which are sufficiently bowed-in  $b$  is actually positive, although quite small for sufficiently large  $z$ , over the entire range of  $z$ . The bowed-out shell has a higher imperfection-sensitivity associated with its considerably higher classical buckling load.

The initial slope of the generalized load-deflection curve of the perfect shell can also be determined from the initial post-buckling analysis. This calculation is given in the Appendix. The resulting pressure vs. effective change in volume relation is

$$\frac{w_{ave}}{w_{oc}} = \frac{\lambda}{\lambda_c} + \frac{1}{\kappa} \left( \frac{\lambda}{\lambda_c} - 1 \right) \quad (9)$$

where  $w_{ave}$  is the average normal displacement of the shell and  $w_{oc}$  is the pre-buckling normal displacement at the critical pressure. The coefficient  $\kappa$ , also calculated in the Appendix, is plotted in Figure 6 as a function of  $z$  for several values of  $r_y/r_x$ .

The results for the lateral pressure buckling of a cylindrical shell ( $r_y/r_x = 0$ ) are in agreement with results obtained previously by Budiansky and Amazigo [4]. The method employed here is the same as that used by these authors. Koiter [5] has determined the initial post-buckling behavior of narrow cylindrical panels under axial compression. Like the toroidal shells considered here the narrow panel has a unique buckling mode and its initial post-buckling behavior is determined by the coefficient  $b$  of the cubic term in Equation (7). Koiter finds that depending on the narrowness of the panel the post-buckling behavior can correspond to either an initially rising or falling load-deflection curve.



TOROIDAL SEGMENTS SUBJECT TO EXTERNAL PRESSURE

In this case there is a prebuckling axial compressive stress in addition to the circumferential stress according to

$$\lambda N_x^0 = -\frac{1}{2} pr_y \quad \text{and} \quad \lambda N_y^0 = -pr_y(1-r_y/2r_x) \quad (10)$$

The results of the classical buckling analysis are shown in Figure 7. The trends are similar to the lateral pressure case although it is noted that the discrepancy between the buckling pressures of the bowed-in and bowed-out shells is emphasized even more.

Plots of  $b/(1-\nu^2)$  vs.  $z$  for different values of  $r_y/r_x$  are shown in Figure 8. As would be expected the shells are more imperfection-sensitive than in the previous case.

When  $r_y/r_x = 1$  the shell is locally spherical at each point on its surface and the prebuckling stresses are exactly those corresponding to a complete spherical shell of similar radius and thickness, namely  $N_x = N_y = -\frac{1}{2} pr$ . The classical buckling pressure of the  $r_y/r_x = 1$  case for large  $z$  is also that for a complete spherical shell

$$p = \frac{2}{\sqrt{3(1-\nu^2)}} E \left(\frac{h}{r}\right)^2$$

Furthermore, when  $r_y/r_x = 1$ , there is not a unique buckling mode, but a large number of buckling modes associated with the classical buckling pressure and the analysis employed in this paper is no longer valid. The multimode post-buckling behavior of a shallow section of a complete spherical shell has been studied in Reference [6]. The spherical shell is a "quadratic type" structure and the buckling load-imperfection relation for small imperfections  $\bar{\xi}$  is of the form

$$1 - \lambda/\lambda_c \approx (a\bar{\xi})^{1/2}$$

while the analogous relation for a "cubic" structure for small  $\bar{\xi}$  is

$$1 - \lambda/\lambda_c \approx (\sqrt{-b} \bar{\xi})^{2/3}$$

The transition from the cubic type structure,  $r_y/r_x < 1$ , to the inherently more imperfection-sensitive quadratic character is reflected in the plots of  $b$  vs.  $z$  for values of  $r_y/r_x$  near unity.

The initial post-buckling behavior of externally pressurized cylindrical shells has also been studied by Budiansky and Amazigo and their results coincide with the  $r_y/r_x = 0$  calculations presented here.

#### TOROIDAL SEGMENTS SUBJECT TO AXIAL TENSION

The prebuckling state of stress in the perfect toroidal shell resulting from an applied axial stress resultant  $N^0$  is

$$\lambda N_x^0 = N^0, \quad \lambda N_y^0 = -N^0 r_y/r_x \quad (11)$$

and a compressive circumferential stress will be induced only if  $r_y/r_x > 0$ . In other words, buckling in tension occurs only for the bowed-out shells. The results of the linear buckling analysis are given in Figure 9 where, now, the buckling parameter is  $K = N^0 l^2 / \pi^2 D$ .

The  $b$  plots, analogous to those of Figures 5 and 8, are presented in Figure 10. Apparently, axial buckling is less influenced by initial shell imperfections than the previous pressure loading cases. If  $r_y/r_x < \frac{1}{2}$  the toroidal segments appear to be relatively insensitive to imperfections. For values of the length parameter less than a certain value, depending on  $r_y/r_x$ ,  $b$  is positive and the load increases in the initial post-buckling region.

Figure 11 gives plots of  $\kappa$  which appears in the load-elongation relation of the perfect shell

$$\frac{\epsilon}{\epsilon_{oc}} = \frac{\lambda}{\lambda_c} + \frac{1}{\kappa} \left( \frac{\lambda}{\lambda_c} - 1 \right) \quad (12)$$

where  $\epsilon$  is the axial elongation and  $\epsilon_{oc}$  is the prebuckling axial elongation at

the critical load. Depending on the value of  $r_y/r_x$  and  $z$ , the slope of the initial post-buckling load elongation curve can be either almost that of the pre-buckling curve or sharply falling. These calculations are given in the Appendix.

Yao [7] compared experimentally obtained buckling loads of axially loaded, truncated hemispheres with predictions based on a linear buckling analysis. The results presented in this section for segments of spheres,  $r_y/r_x = 1$ , are not directly applicable since both Yao's calculations and the tests correspond to clamped end conditions. On the other hand, qualitative agreement should be expected with respect to the degree of imperfection-sensitivity of clamped and simply supported shells. The test specimens were sufficiently short (i.e.,  $l/r_x$  sufficiently small) to justify, if only approximately, the shallowness assumption made in the present analysis. The test buckling loads ranged from one third to slightly over one half the classical buckling loads with the length parameters falling in the range  $50 < z < 160$ . It is interesting to note that the range of the  $z$ 's of the test specimens falls within the imperfection-sensitive range predicted by the present analysis.

#### APPENDIX: INITIAL POST-BUCKLING CALCULATIONS

##### DONNELL-TYPE NONLINEAR SHELL EQUATIONS

The membrane strains  $\epsilon_x$ ,  $\epsilon_y$  and  $\epsilon_{xy}$  of Donnell-type theory are related to the normal and tangential displacements to the shell middle surface  $w$ ,  $u$ ,  $v$  by

$$\begin{aligned}\epsilon_x &= u_{,x} + w/r_x + \frac{1}{2} w^2_{,x} + \bar{w}_{,x} w_{,x} \\ \epsilon_y &= v_{,y} + w/r_y + \frac{1}{2} w^2_{,y} + \bar{w}_{,y} w_{,y}\end{aligned}\tag{13}$$

and

$$2\epsilon_{xy} = v_{,x} + u_{,y} + w_{,x} w_{,y} + \bar{w}_{,x} w_{,y} + w_{,x} \bar{w}_{,y}$$

where  $\bar{w}$  is the initial normal deflection of the shell middle surface from the perfect toroidal segment with radii  $r_x$  and  $r_y$ . The bending strain-displacement relations are linear:  $k_x = -w_{,xx}$ ,  $k_y = -w_{,yy}$  and  $k_{xy} = -w_{,xy}$ . The stress-strain relations are also linear:  $E\epsilon_x = N_x - \nu N_y$ ,  $M_x = D(k_x + \nu k_y)$ , etc.

Equations of equilibrium can be formulated in terms of a variational principle of virtual work. For Donnell theory the statement of this principle is

$$\int_S (N_x \delta\epsilon_x + N_y \delta\epsilon_y + 2N_{xy} \delta\epsilon_{xy} + M_x \delta k_x + M_y \delta k_y + 2M_{xy} \delta k_{xy}) dS + \int_S \lambda p^0 \delta w dS - \int_C \lambda N^0 \delta u ds = 0 \quad (14)$$

where  $\lambda p^0$  is the applied pressure,  $\lambda N^0$  is the stress resultant applied at the ends of the shell and  $\delta\epsilon_x = \delta u_{,x} + \delta w/r_x + w_{,x} \delta w_{,x} + \bar{w}_{,x} \delta w_{,x}$ ,  $\delta k_x = -\delta w_{,xx}$ , etc. The scalar load parameter  $\lambda$  has been introduced to emphasize that for each loading combination considered in this paper the axial load and lateral pressure are fixed in a definite ratio. Thus,  $N^0$  and  $p^0$  are assumed fixed in a manner appropriate to the particular loading combination. The differential equations associated with this variational principle are the three equilibrium equations, which when expressed in terms of the three displacements  $u$ ,  $v$ ,  $w$ , provide the set of Donnell-type equations governing the deformation of the shell. Boundary conditions in this analysis are taken to be  $v = w = M_x = 0$  and  $N_x = \lambda N^0$  at the ends of the shell,  $x = 0, l$ .

The prebuckling stresses in the perfect shell for a given lateral pressure loading  $\lambda p^0$  and applied axial stress  $\lambda N^0$  are uniform, except for deviations in a narrow region near the ends of the shell which will be neglected in this analysis. The nonzero prebuckling stresses and deformations are

$$\lambda N_x^0 = \lambda N^0, \quad \lambda N_y^0 = -\lambda(p^0 r_y + N^0 r_y / r_x) \quad (15)$$

$$\lambda w^0 = - \frac{\lambda r_y}{Eh} [N^0 (r_y/r_x + \nu) + p^0 r_y]$$

(16)

and

$$\lambda u^0_{,x} = \frac{\lambda}{Eh} [N^0 ((r_y/r_x)^2 + 2\nu r_y/r_x + 1) + p^0 r_y (r_y/r_x + \nu)]$$

INITIAL POST-BUCKLING ANALYSIS FOR UNIQUE MODE BUCKLING

The notation and development of Koiter's general theory displayed here are taken from Reference [8]. Only the outline and essential results of the theory will be given. The reader is referred to Reference [8] or Koiter's own work [1] for omitted details and points of rigor which will not be re-established here. For brevity, the stress, strain and displacement fields are denoted by  $\sigma$ ,  $\epsilon$  and  $u$ , respectively.† The magnitude of the applied load system is taken to be directly proportional to the load parameter  $\lambda$ .

The strain-displacement relations of the perfect shell are written symbolically as

$$\epsilon = L_1(u) + \frac{1}{2} L_2(u) \tag{17}$$

where  $L_1$  and  $L_2$  are, then, homogeneous functionals which are linear and quadratic, respectively, in  $u$ . In the presence of an initial deflection of the unloaded structure  $\bar{u}$  the strain resulting from an additional displacement  $u$  is

$$\epsilon = L_1(u) + \frac{1}{2} L_2(u) + L_{11}(u, \bar{u}) \tag{18}$$

where  $L_{11}(u, \bar{u}) = L_{11}(\bar{u}, u)$  is the bilinear, homogeneous functional of  $u$  and  $\bar{u}$  which appears in the identity

$$L_2(u + \bar{u}) = L_2(u) + 2L_{11}(u, \bar{u}) + L_2(\bar{u})$$

The stress-strain relations are linear and are denoted by

---

† In the general development  $u$  is a generalized expression for the displacements. It should not be confused with the axial displacement in the Donnell theory which bears the same symbol.

$$\sigma = H_1(\epsilon) \quad (19)$$

where  $H_1$  is a homogeneous, linear functional.

Equations of equilibrium are formulated via the principle of virtual work.

In compact form this principle (Equation (14) for Donnell theory) is written as

$$\{\sigma, \delta\epsilon\} - \lambda B_1(\delta u) = 0 \quad (20)$$

where  $\{\sigma, \delta\epsilon\}$  is the internal virtual work of the stress field  $\sigma$  through the strain variation  $\delta\epsilon$  and  $\lambda B_1(\delta u)$  is the external virtual work of the load system of intensity  $\lambda$  through the admissible displacement variation  $\delta u$ .

The prebuckling deformations of the perfect shells, Equation (16), are linearly dependent on the applied load and are abbreviated as  $\lambda u_0$ . Since the prebuckling strains are linearly dependent on the displacements, i.e.,  $L_2(u_0) = 0$ , the prebuckling stresses, Equation (15), are denoted by  $\lambda \sigma^0$  and are related to  $\lambda u_0$  by  $\sigma^0 = H_1[L_1(u_0)]$ . To discover the eigenvalue  $\lambda_c$  and eigenmode  $u_c$  for classical buckling we set

$$u = \lambda_c u_0 + u_c$$

in the field equations and retain only the linear terms in the buckling mode  $u_c$ .

The resulting variational equation is, in the compact notation,

$$\lambda_c \{\sigma_0, L_{11}(u_c, \delta u)\} + \{s_c, L_1(\delta u)\} = 0 \quad (21)$$

where  $s_c = L_1(u_c)$ . When this statement is translated into Donnell notation the differential equations associated with this variational equation are the linear buckling equations which, when written in terms of a stress function and the normal displacement in the usual manner, become Equations (1) and (2).

As previously mentioned, each structure-loading combination investigated in this paper has a unique buckling mode associated with the classical buckling load. To study the initial post-buckling behavior one writes the total displacement, quite generally, as

$$u = \lambda u_0 + \xi u_c + \tilde{u} \quad (22)$$

where  $u_c$  is now considered normalized in magnitude in a definite way. The displacement  $\tilde{u}$  is taken to be orthogonal to  $u_c$  in the sense

$$\{\sigma_0, L_{11}(u_c, \tilde{u})\} = 0 \quad (23)$$

When a structure is imperfection-sensitive, imperfections in the form of the buckling mode are most critical. In this study the imperfection is taken as

$$\bar{u} = \bar{\xi} u_c \quad (24)$$

The initial post-buckling analysis provides an algebraic equilibrium equation relating  $\xi$ ,  $\bar{\xi}$  and the load parameter  $\lambda$ . This equation is a representation which is uniformly valid for small  $\xi$  and  $\bar{\xi}$ . To obtain this equation one writes

$$\begin{aligned} \tilde{u} = & \xi^2 u_2 + \xi^3 u_3 + \dots \\ & + \bar{\xi} [\xi u_{11} + \xi^2 u_{21} + \dots] + \dots \end{aligned} \quad (25)$$

and then  $u$  as given by (22), with the aid of Equations (17)-(19), is substituted into the variational equilibrium equation. The requirement that Equation (20) be satisfied for the variation  $\delta u = u_c \delta \xi$  gives the scalar equation relating  $\lambda$  to  $\xi$  and  $\bar{\xi}$

$$\begin{aligned} & -\xi(\lambda_c - \lambda) \{\sigma_0, L_2(u_c)\} + \frac{3}{2} \xi^2 \{s_c, L_2(u_c)\} \\ & + \xi^3 [2\{s_c, L_{11}(u_c, u_2)\} + \{s_2, L_2(u_c)\} + \frac{1}{2} \{H_1(L_2(u_c)), L_2(u_c)\}] \\ & + O(\xi^4) + \dots = -\bar{\xi} \lambda \{\sigma_0, L_2(u_c)\} + O(\bar{\xi} \bar{\xi}, \bar{\xi}^2) + \dots \end{aligned} \quad (26)$$

where  $s_c = L_1(u_c)$  and  $s_2 = L_1(u_2)$ . For all variations  $\delta u$  orthogonal to  $u_c$ , Equation (20) provides the variational equation necessary for determining  $u_2$

$$\begin{aligned} \lambda_c \{\sigma_0, L_{11}(u_2, \delta u)\} + \{s_2, L_1(\delta u)\} = \\ - \{s_c, L_{11}(u_c, \delta u)\} - \frac{1}{2} \{H_1[L_2(u_c)], L_1(\delta u)\} \end{aligned} \quad (27)$$

Equation (26) can be written in the form of Equation (6) given in the body of the report, i.e.,

$$\left(1 - \frac{\lambda}{\lambda_c}\right)\xi + a\xi^2 + b\xi^3 + \dots = \frac{\lambda}{\lambda_c} \bar{\xi} + \dots \quad (6)$$

where the coefficients  $a$  and  $b$  are

$$a = \frac{\frac{3}{2}\{s_{c,L_2}(u_c)\}}{-\lambda_c\{\sigma_{0,L_2}(u_c)\}} \quad (28)$$

and

$$b = \frac{2\{s_{c,L_{11}}(u_c, u_2)\} + \{s_{2,L_2}(u_c)\} + \frac{1}{2}\{H_1[L_2(u_c)], L_2(u_c)\}}{-\lambda_c\{\sigma_{0,L_2}(u_c)\}} \quad (29)$$

#### CALCULATION OF THE $b$ COEFFICIENT FOR TOROIDAL SHELL SEGMENTS

The buckling mode (4) is such that the  $\lambda$  vs.  $\xi$  relation of the perfect toroidal shell can depend only on the magnitude of  $\xi$  and not on its sign and, thus,  $a$  must be zero. This can be verified directly by noting that

$$\begin{aligned} \{s_{c,L_2}(u_c)\} &= \int_S (f_{c,yy} w_{c,x}^2 + f_{c,xx} w_{c,y}^2 - 2f_{c,xy} w_{c,x} w_{c,y}) dS \\ &= 0 \end{aligned}$$

where, consistent with Equation (4),

$$\begin{aligned} w_c &= h \sin(\pi x/\ell) \sin(ny/r_y) \\ f_c &= -\frac{Eh^2 \ell^2 A}{\pi^2 r_y} \sin(\pi x/\ell) \sin(ny/r_y) \end{aligned} \quad (30)$$

and

$$A = \left[ \frac{1 + \bar{n}^2 r_y / r_x}{(1 + \bar{n}^2)^2} \right]$$

The initial post-buckling behavior, then, is determined by  $b$  as long as this coefficient does not also vanish. Evaluation of  $b$  necessitates solving for  $u_2$ . A straightforward translation of the variational Equation (27) into Donnell



notation followed by the usual calculus of variations procedure leads to three simultaneous partial differential equations for  $u_2$ ,  $v_2$  and  $w_2$ . These equations are

$$\begin{aligned} D\nabla^4 w_2 + \frac{1}{r_x} N_x^{(2)} + \frac{1}{r_y} N_y^{(2)} - \lambda_c N_c^0 w_{2,xx} - \lambda_c N_c^0 w_{2,yy} &= f_{c,yy} w_{c,xx} + f_{c,xx} w_{c,yy} - \\ &- 2f_{c,xy} w_{c,xy} - \frac{1}{2} \frac{Eh}{1-\nu^2} \left[ \frac{1}{r_x} (w_{c,x}^2 + \nu w_{c,y}^2) + \frac{1}{r_y} (w_{c,y}^2 + \nu w_{c,x}^2) \right] \\ N_{x,x}^{(2)} + N_{xy,y}^{(2)} &= -\frac{1}{2} \frac{Eh}{1-\nu^2} \left[ (w_{c,x}^2 + \nu w_{c,y}^2)_{,x} + (1-\nu) (w_{c,x} w_{c,y})_{,y} \right] \\ N_{y,y}^{(2)} + N_{xy,x}^{(2)} &= -\frac{1}{2} \frac{Eh}{1-\nu^2} \left[ (w_{c,y}^2 + \nu w_{c,x}^2)_{,y} + (1-\nu) (w_{c,x} w_{c,y})_{,x} \right] \end{aligned}$$

with the boundary conditions  $w_2 = w_{2,xx} = v_2 = 0$  and  $N_x^{(2)} + \frac{1}{2} [Eh/(1-\nu^2)] [w_{c,x}^2 + \nu w_{c,y}^2] = 0$  at  $x = 0, l$ , where  $N_x^{(2)} = \frac{Eh}{1-\nu^2} [u_{2,x} + w_2/r_x + \nu(v_{2,y} + w_2/r_y)]$ , etc.

These equations are reduced to a much more manageable form if the stress function  $f_2$  is introduced according to

$$\begin{aligned} N_x^{(2)} &= f_{2,yy} - \frac{1}{2} \frac{Eh}{1-\nu^2} (w_{c,x}^2 + \nu w_{c,y}^2) \\ N_y^{(2)} &= f_{2,xx} - \frac{1}{2} \frac{Eh}{1-\nu^2} (w_{c,y}^2 + \nu w_{c,x}^2) \\ N_{xy}^{(2)} &= -f_{2,xy} - \frac{1}{2} \frac{Eh}{1+\nu} w_{c,x} w_{c,y} \end{aligned}$$

Then the equations for  $w_2$  and  $f_2$  become

$$\begin{aligned} D\nabla^4 w_2 + \frac{1}{r_y} f_{2,xx} + \frac{1}{r_x} f_{2,yy} - \lambda_c N_c^0 w_{2,xx} - \lambda_c N_c^0 w_{2,yy} \\ = f_{c,yy} w_{c,xx} + f_{c,xx} w_{c,yy} - 2f_{c,xy} w_{c,xy} \end{aligned} \quad (31)$$

and, secondly, the compatibility equation

$$\frac{1}{Eh} \nabla^4 f_2 - \frac{1}{r_y} w_{2,xx} - \frac{1}{r_x} w_{2,yy} = w_{c,xy}^2 - w_{c,xx} w_{c,yy} \quad (32)$$

and the boundary conditions reduce to

$$w_2 = w_{2,xx} = f_{2,xx} = f_2 = 0 \quad \text{at} \quad x = 0, \ell$$

A stress function has been introduced and, thus, a further condition is that the tangential displacements be single valued over a complete circuit of the shell.

For  $v_2$  this condition is equivalent to

$$\int_0^{2\pi r_y} \left[ \frac{1}{Eh} (f_{2,xx} - \nu f_{2,yy}) - \frac{1}{2} w_{c,y}^2 - \frac{w_2}{r_y} \right] dy = 0 \quad (33)$$

The right hand sides of Equations (31) and (32) are respectively,

$$-\frac{Eh^3 A (\bar{n}\pi/\ell)^2}{r_y} (\cos(2\pi x/\ell) + \cos(2ny/r_y)) \quad \text{and} \quad \frac{1}{2} h^2 \bar{n}^2 (\pi/\ell)^4 (\cos(2\pi x/\ell) + \cos(2ny/r_y)) .$$

The solution to Equations (31) and (32) can be written in the separated form

$$w_2 = \sum_{i=1,3,5,\dots}^{\infty} \alpha_i \sin(i\pi x/\ell) + \cos(2ny/r_y) \sum_{i=1,3,5,\dots}^{\infty} \gamma_i \sin(i\pi x/\ell) \quad (34)$$

and

$$f_2 = \sum \beta_i \sin(i\pi x/\ell) + \cos(2ny/r_y) \sum \delta_i \sin(i\pi x/\ell) \quad (35)$$

and the coefficients of these series can be determined with the Galerkin procedure. One finds

$$\alpha_i = \pi(1-\nu^2)^{1/2} \bar{n}^2 h \bar{\alpha}_i = \pi(1-\nu^2)^{1/2} \bar{n}^2 h (A i^2 + 1/2) / Q_i$$

$$\beta_i = \pi \bar{n}^2 E h^3 \bar{\beta}_i = \pi \bar{n}^2 E h^3 (\pi^2 i^2 / 24z + \lambda \bar{N}_c^0 / 2 - A z / \pi^2) / Q_i$$

$$\gamma_i = 4\pi(1-\nu^2)^{1/2} \bar{n}^2 h \bar{\gamma}_i = 4\pi(1-\nu^2)^{1/2} \bar{n}^2 h [A(i^2 + 4\bar{n}^2)^2 + i^2/2 + 2\bar{n}^2 r_y / r_x] / H_i$$

$$\delta_i = 4\pi \bar{n}^2 E h^3 \bar{\delta}_i = 4\pi \bar{n}^2 E h^3 [\pi^2 (i^2 + 4\bar{n}^2)^2 / 24z + \lambda \bar{N}_c^0 i^2 / 2$$

$$+ 2\lambda \bar{N}_c^0 \bar{n}^2 - z(i^2 + 4\bar{n}^2 r_y / r_x) A / \pi^2] / H_i$$

$$i = 1, 3, 5 \dots$$

with

$$Q_1 = i(i^2-4)(\pi^4 i^4/12z + \lambda_c \bar{N}_x^0 \pi^2 i^2 + z)/4$$

$$H_1 = i[\pi^4(i^2+4\bar{n}^2)^4/12z + \lambda_c \bar{N}_x^0 \pi^2 i^2 (i^2+4\bar{n}^2)^2 + \lambda_c \bar{N}_y^0 4\pi^2 \bar{n}^2 (i^2+4\bar{n}^2)^2 + z(i^2+4\bar{n}^2 r_y/r_x)^2]$$

and where  $\lambda_c \bar{N}_x^0 = \lambda_c (1-\nu^2)^{1/2} r_y N_x^0/Eh^2$  and  $\lambda_c \bar{N}_y^0 = \lambda_c (1-\nu^2)^{1/2} r_x N_y^0/Eh^2$ .

That this solution satisfies the single valued conditions can be verified by direct substitution into Equation (33), for example. Alternatively one notes immediately that the  $y$  dependent terms in (34) and (35) satisfy Equation (33). Then one can recognize that Equation (32), for the  $y$  independent part of the solution, when integrated twice with respect to  $x$  in conjunction with the boundary conditions is precisely condition (33). Similarly one can show that  $u_2$  is single valued.

Now,  $b$  can be calculated using Equation (29) if it is noted that

$$-\lambda_c \{ \sigma_0, L_2(u_c) \} = -\lambda_c \int_S (N_x^0 w_{c,x}^2 + N_y^0 w_{c,y}^2) dS$$

$$\begin{aligned} \{ s_c, L_{11}(u_c, u_2) \} &= \int_S [f_{c,yy} w_{c,x} w_{2,x} + f_{c,xx} w_{c,y} w_{2,y} \\ &\quad - f_{c,xy} (w_{c,x} w_{2,y} + w_{c,y} w_{2,x})] dS \end{aligned}$$

and

$$\{ s_2, L_2(u_c) \} + \frac{1}{2} \{ H_1[L_2(u_c)], L_2(u_c) \} =$$

$$\int_S (f_{2,yy} w_{c,x}^2 + f_{2,xx} w_{c,y}^2 - 2f_{2,xy} w_{c,x} w_{c,y}) dS$$

The results of this calculation are

$$b = \frac{-8(1-\nu^2)\bar{n}^4}{\lambda_c (\bar{N}_x^0 + \bar{N}_y^0 \bar{n}^2)} \left[ (\sum \bar{\beta}_i \frac{1}{(i^2-4)} + 2\sum \bar{\delta}_i \frac{1}{i}) \pi^2/z \right. \\ \left. - 2A (\sum \bar{\alpha}_i \frac{1}{(i^2-4)} + 2\sum \bar{\gamma}_i \frac{1}{i}) \right] \quad (36)$$

For the three loading cases presented in this paper the  $b$  calculations were made with the aid of a digital computer. The series in Equation (36) were evaluated by taking a sufficiently large number of terms to insure that the truncation error was less than 1/10 of one percent.

The generalized load-deflection relation for the lateral pressure case was calculated directly from the expression for the total normal displacement

$$w = \lambda w_0 + \xi w_c + \xi^2 w_2 + \dots$$

Since  $\int w_c dS = 0$  and  $\xi^2 = -(1-\lambda/\lambda_c)/b$ , the initial post-buckling load-deflection relation between the average lateral deflection of the perfect shell and the lateral pressure is

$$\frac{w_{ave}}{w_{oc}} = \frac{\lambda}{\lambda_c} + \eta \left(1 - \frac{\lambda}{\lambda_c}\right) \quad (37)$$

where  $w_{oc} = \lambda_c w_0$  is the prebuckling displacement at the critical pressure and

$$\eta = \frac{-1}{2\pi r_y \ell b w_{oc}} \int_S w_2 dS$$

This coefficient was calculated using a series representation, not given here, which was obtained from the expression for  $w_2$ , Equation (34). It is more convenient to rewrite Equation (37) in the form given in the body of the paper, namely,

$$\frac{w_{ave}}{w_{oc}} = \frac{\lambda}{\lambda_c} + \frac{1}{\kappa} \left( \frac{\lambda}{\lambda_c} - 1 \right) \quad (9)$$

where  $\kappa = -1/\eta$ . Plots of  $\kappa$  as a function of  $z$  for several values of

$r_y/r_x$  are given in Figure 6. Neglection of the distortion of the shell near its ends places the same limitation on the load-deflection relation and buckling load-imperfection relation as has been remarked on previously with regard to the classical buckling analysis.

In a similar fashion the axial load-elongation relation for the initial post-buckling regime of a perfect shell in axial tension can be calculated directly.

The average elongation is

$$\epsilon = \frac{1}{2\pi r} \int_S \left[ \frac{1}{Eh} (N_x - \nu N_y) - \frac{w}{r_x} - \frac{1}{2} w_{,x}^2 \right] dS$$

The parameter in the load-deflection relation, Equation (12), is again

$\kappa = -1/\eta$  where now

$$\eta = \frac{-1}{2\pi r b \epsilon_{oc}} \int_S \left[ \frac{1}{Eh} (f_{2,yy} - \nu f_{2,xx}) - \frac{w_2}{r_x} - \frac{1}{2} w_{c,x}^2 \right] dS$$

and  $\epsilon_{oc}$  is the axial elongation at the onset of buckling. A series representation for  $\eta$  is obtained in a straightforward way. The results of the calculations are shown in Figure 11 as plots of  $\kappa$  vs.  $z$ .

REFERENCES

1. Koiter, W. T., "Elastic Stability and Post-buckling Behavior", Proc. Symp. "Nonlinear Problems", edited by R. E. Langer, Univ. of Wisc. Press, p. 257 (1963).
2. Stein, M. and McElman, J. A., "Buckling of Segments of Toroidal Shells", AIAA J., 3, 1704-10 (1965).
3. Almroth, B. O., "Influence of Edge Conditions on the Stability of Axially Compressed Cylindrical Shells", NASA Contract Rept. 161 (1965).
4. Budiansky, B. and Amazigo, J., Private communication on initial post-buckling behavior of externally pressurized cylindrical shells, to be published (1965).
5. Koiter, W. T., "Buckling and Post-buckling Behavior of a Cylindrical Panel under Axial Compression", Report S. 476, Nat. Aero. Research Inst., Amsterdam (1956).
6. Hutchinson, J. W., "Imperfection-Sensitivity of Externally Pressurized Spherical Shells", Report SM-5, Harvard University (1965).
7. Yao, J. C., "Buckling of a Truncated Hemisphere under Axial Tension", AIAA J., 1, 2316-20 (1963).
8. Budiansky, B. and Hutchinson, J., "Dynamic Buckling of Imperfection-Sensitive Structures", Proc. of the Eleventh International Cong. of Applied Mech. (1964). (Springer: Julius Springer-Verlag, Berlin, to be published.)

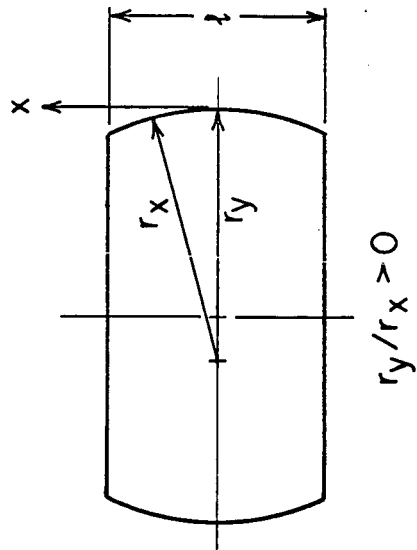
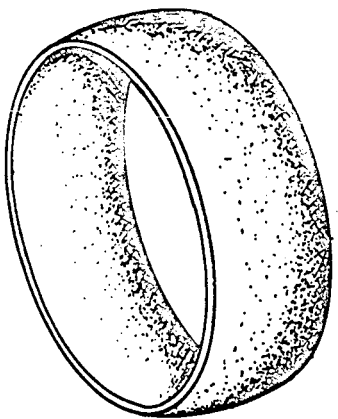
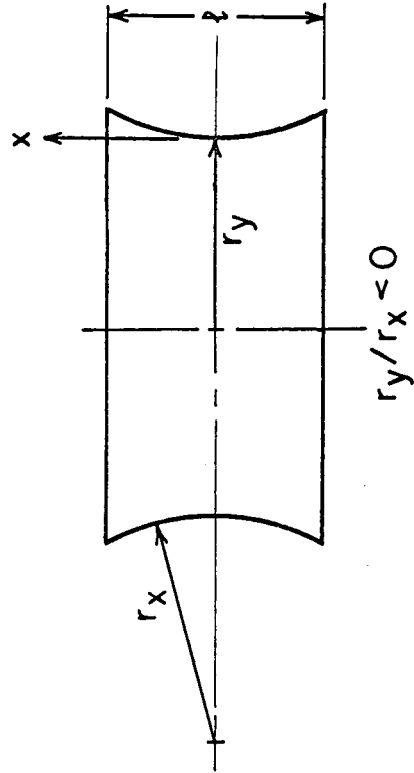
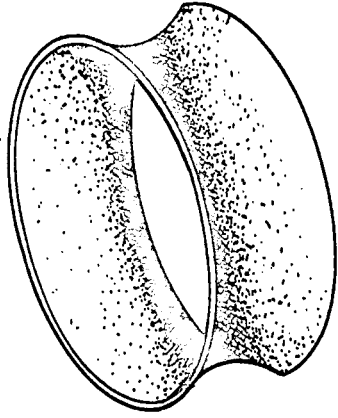


FIG. 1 CONFIGURATION OF TOROIDAL SEGMENTS

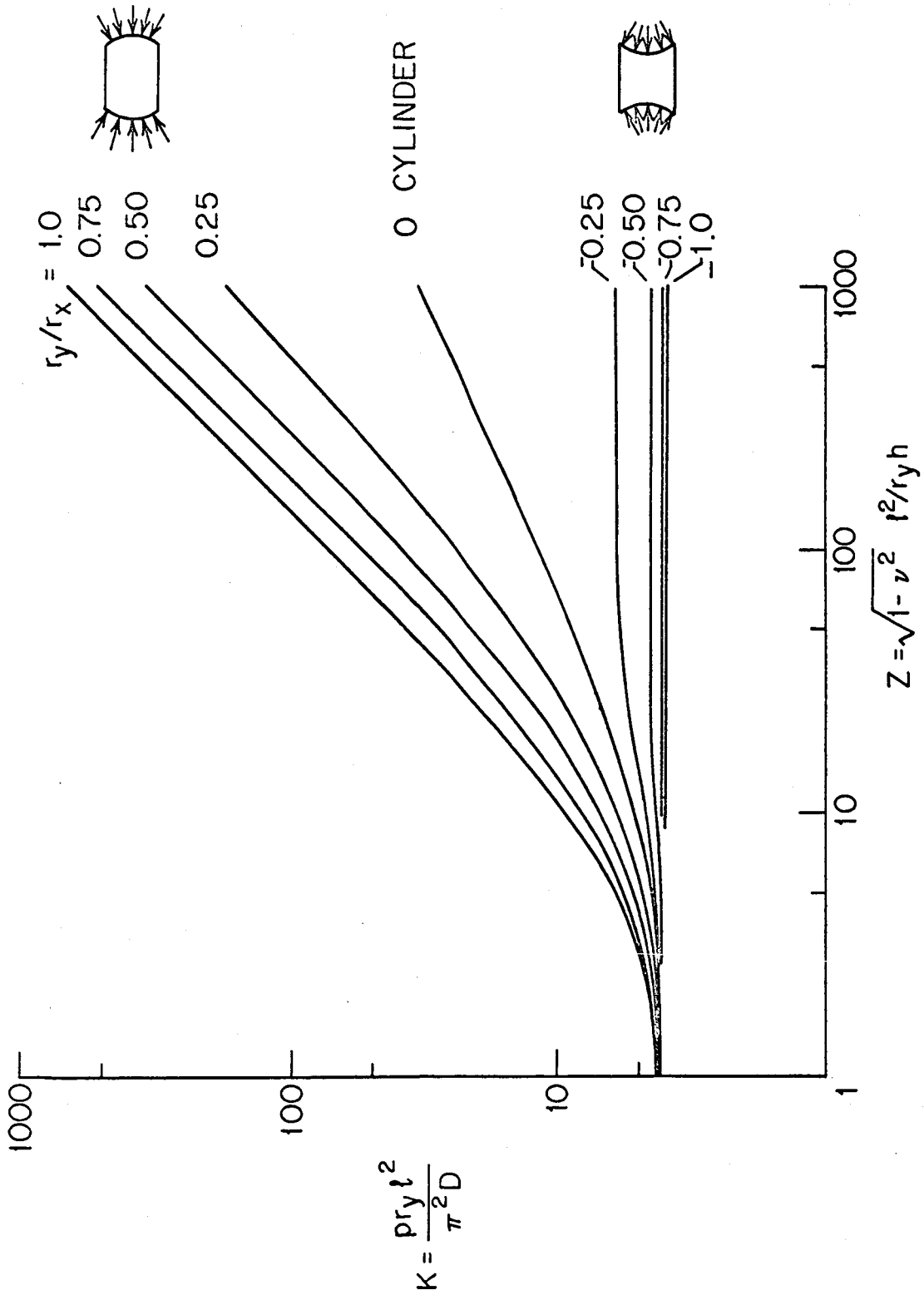


FIG. 2 CLASSICAL BUCKLING OF TOROIDAL SEGMENTS UNDER LATERAL PRESSURE



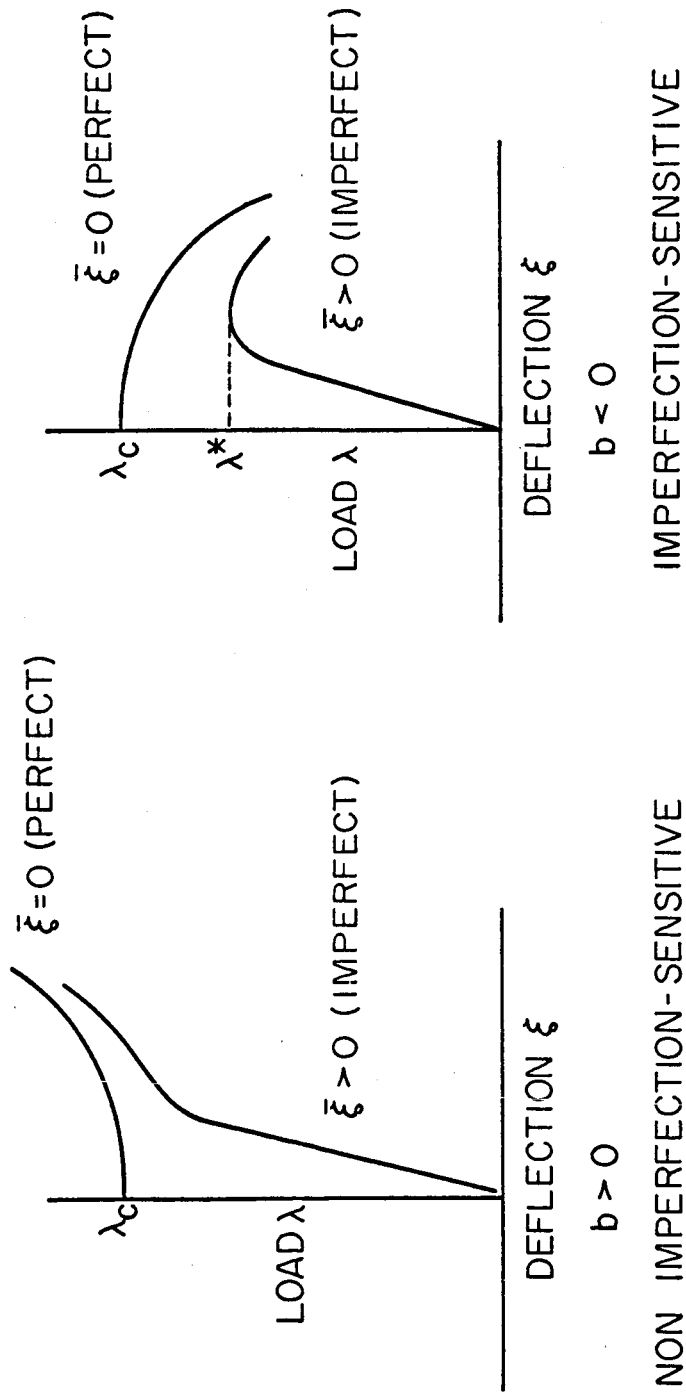


FIG. 3 LOAD-DEFLECTION BEHAVIOR OF CUBIC STRUCTURE

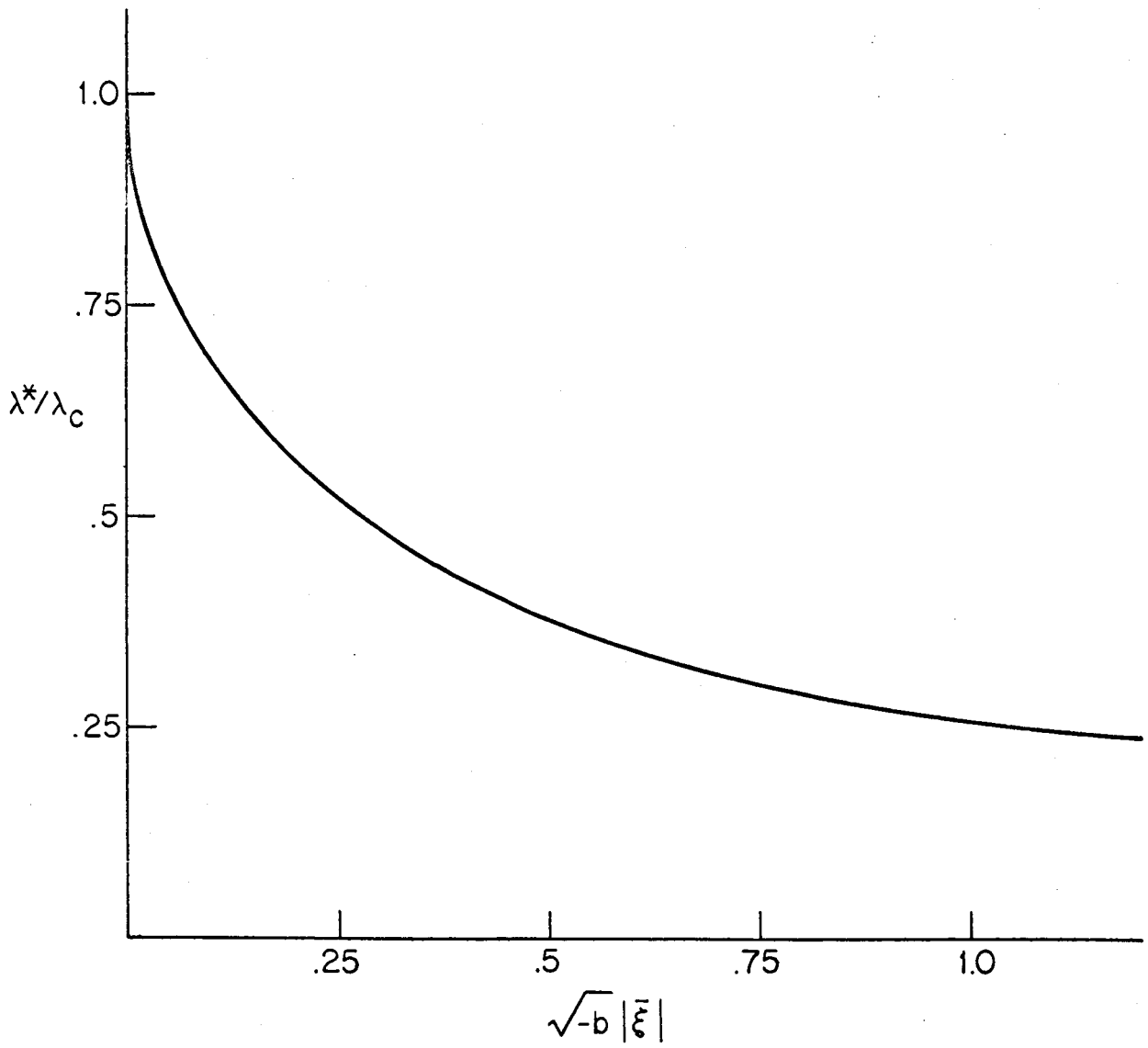


FIG. 4 BUCKLING LOAD vs. IMPERFECTION RELATION

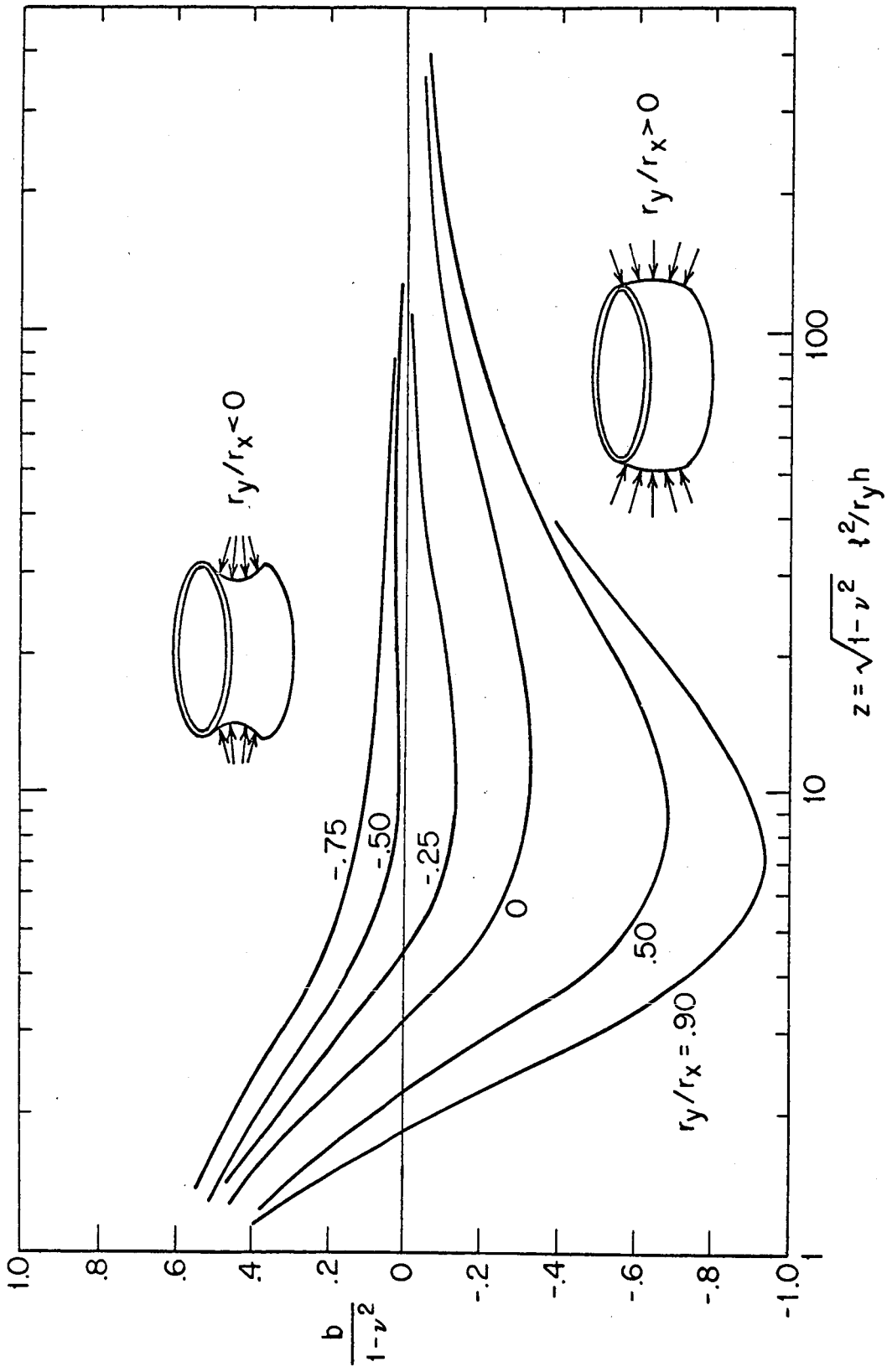


FIG. 5 INITIAL POST-BUCKLING COEFFICIENT FOR LATERAL PRESSURE CASE

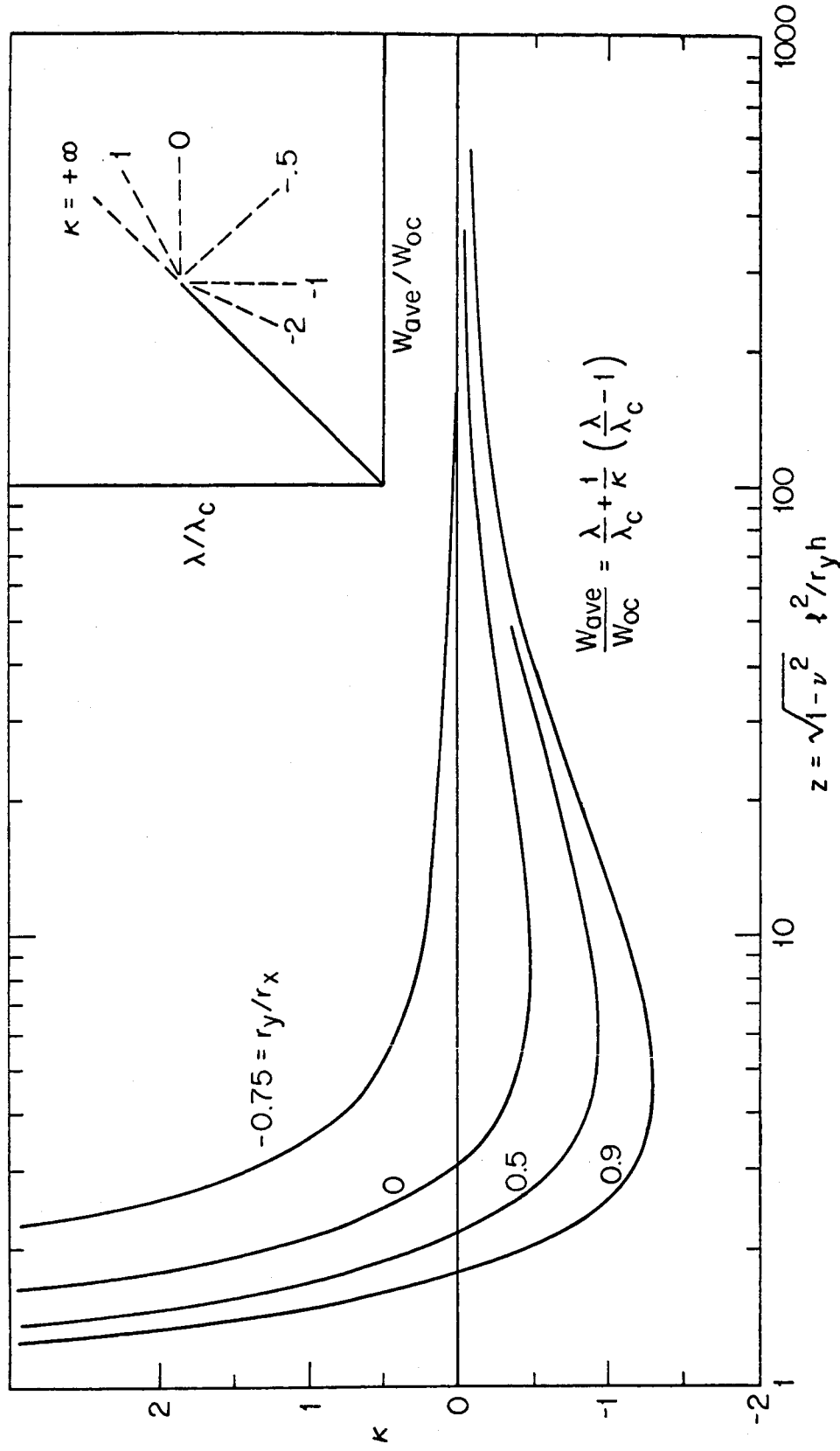


FIG. 6 INITIAL POST-BUCKLING PRESSURE - LATERAL DEFLECTION RELATION

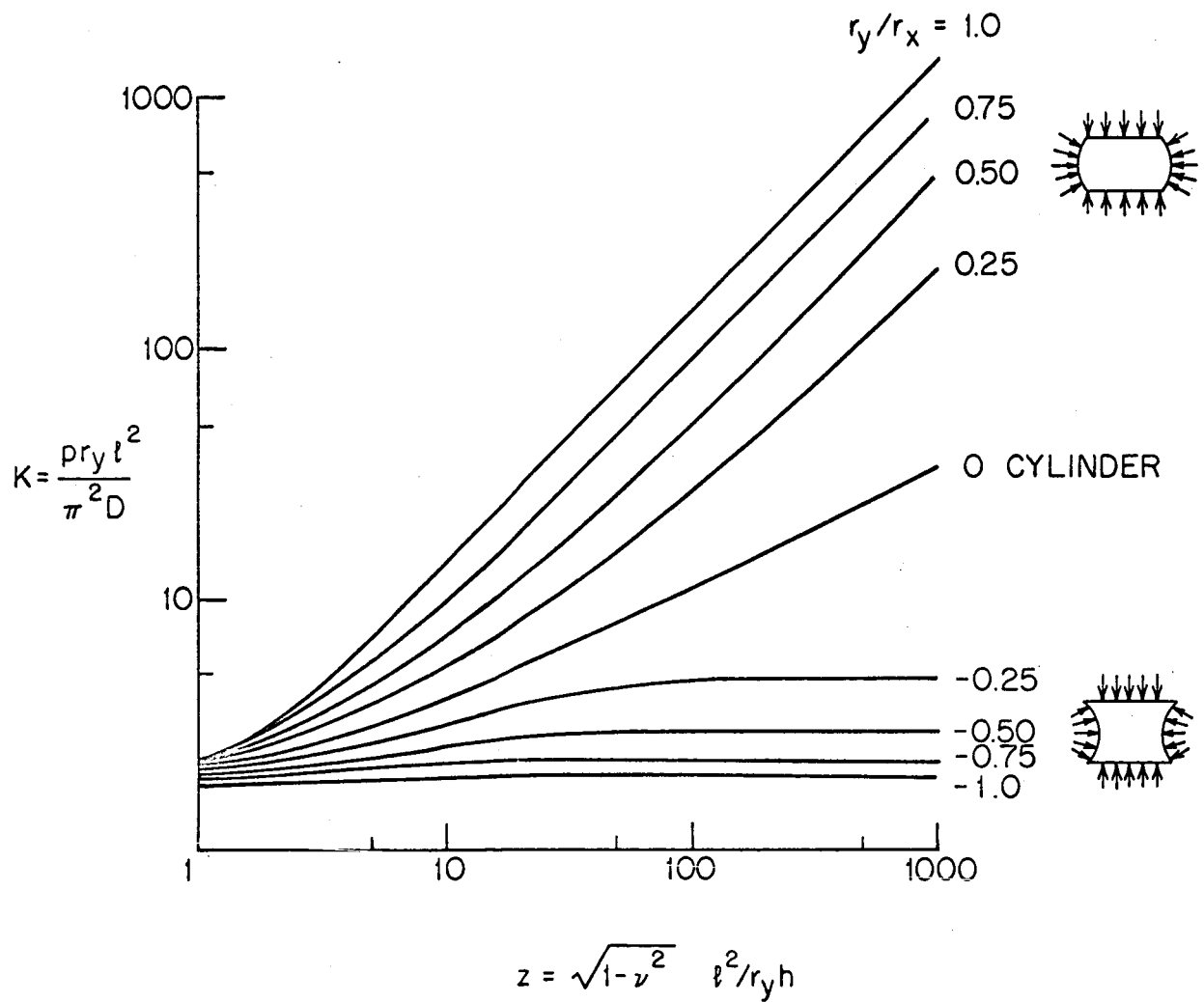


FIG. 7 CLASSICAL BUCKLING OF TOROIDAL SEGMENTS UNDER EXTERNAL HYDROSTATIC PRESSURE

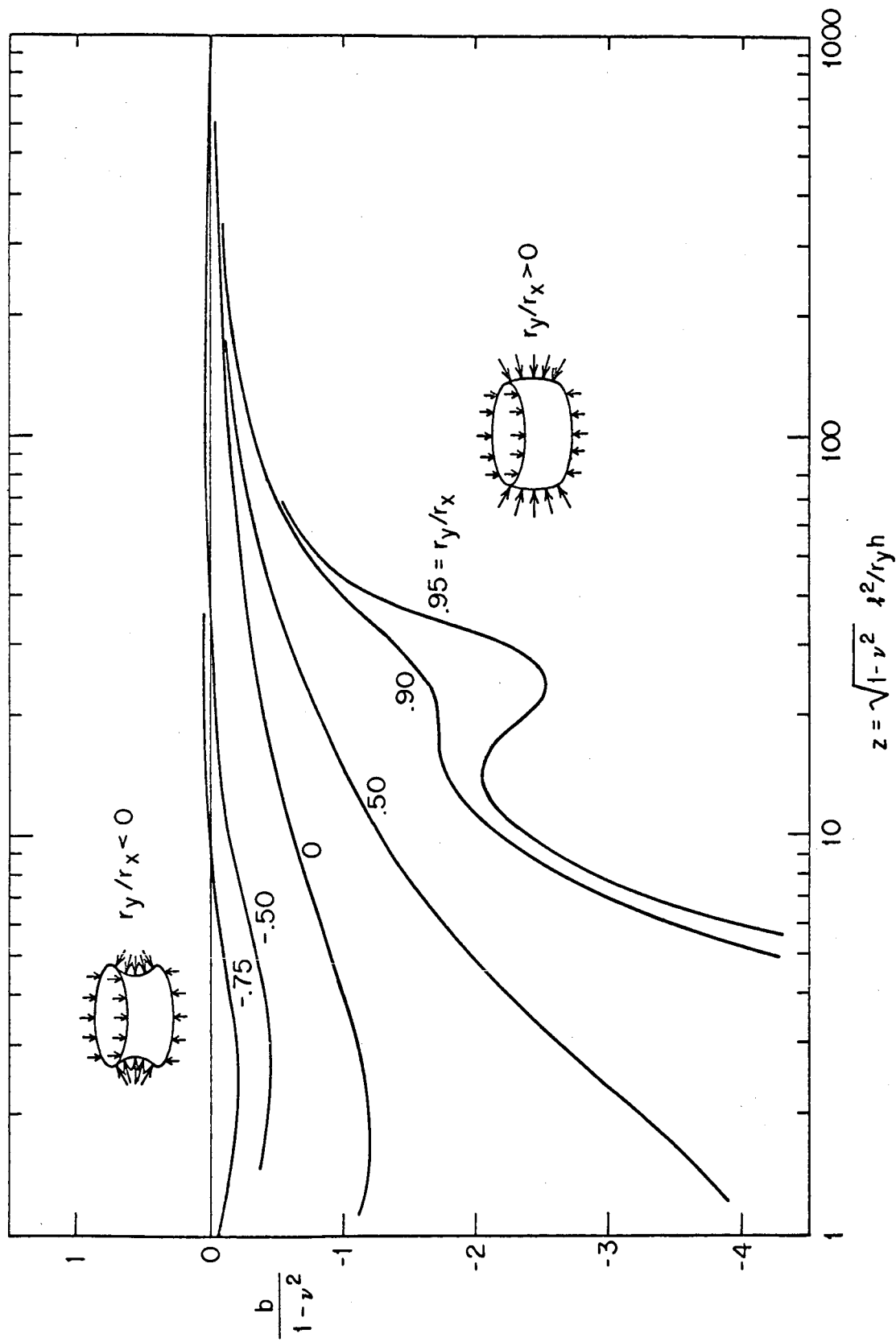


FIG. 8 INITIAL POST-BUCKLING COEFFICIENT FOR EXTERNAL PRESSURE CASE

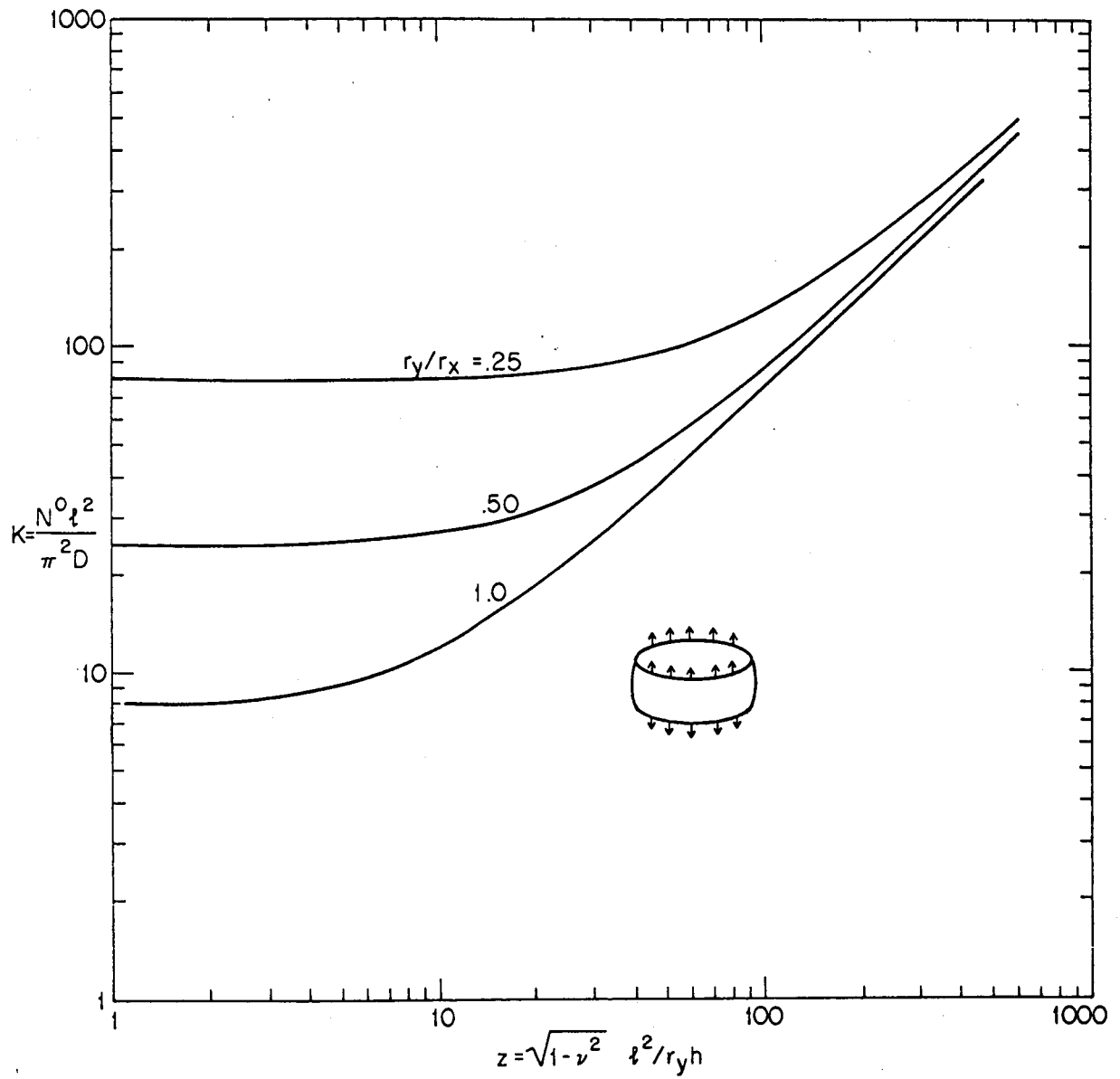


FIG. 9 CLASSICAL BUCKLING OF BOWED-OUT TOROIDAL SEGMENTS UNDER AXIAL TENSION

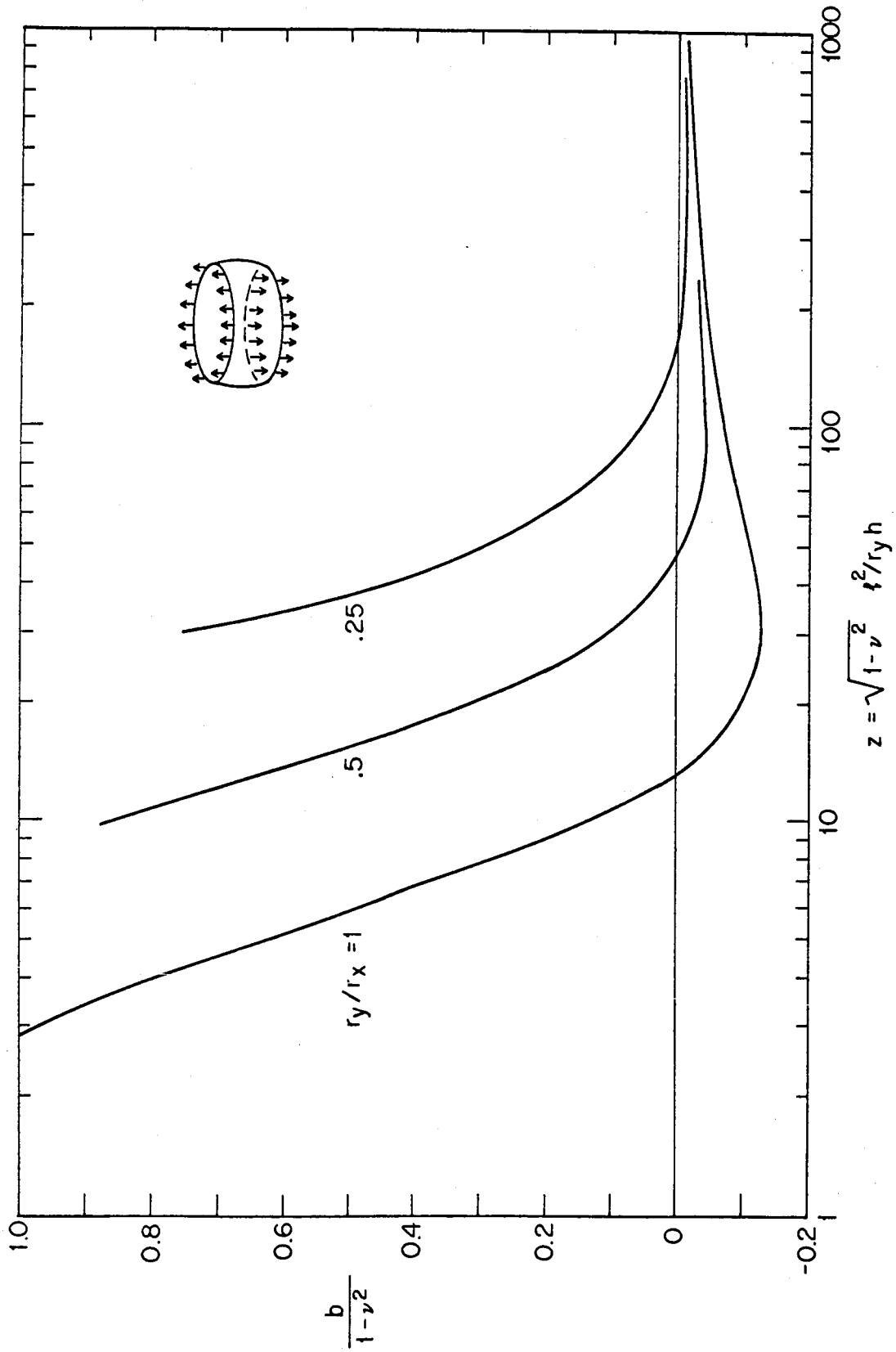


FIG. 10 INITIAL POST-BUCKLING COEFFICIENT FOR BUCKLING UNDER AXIAL TENSION



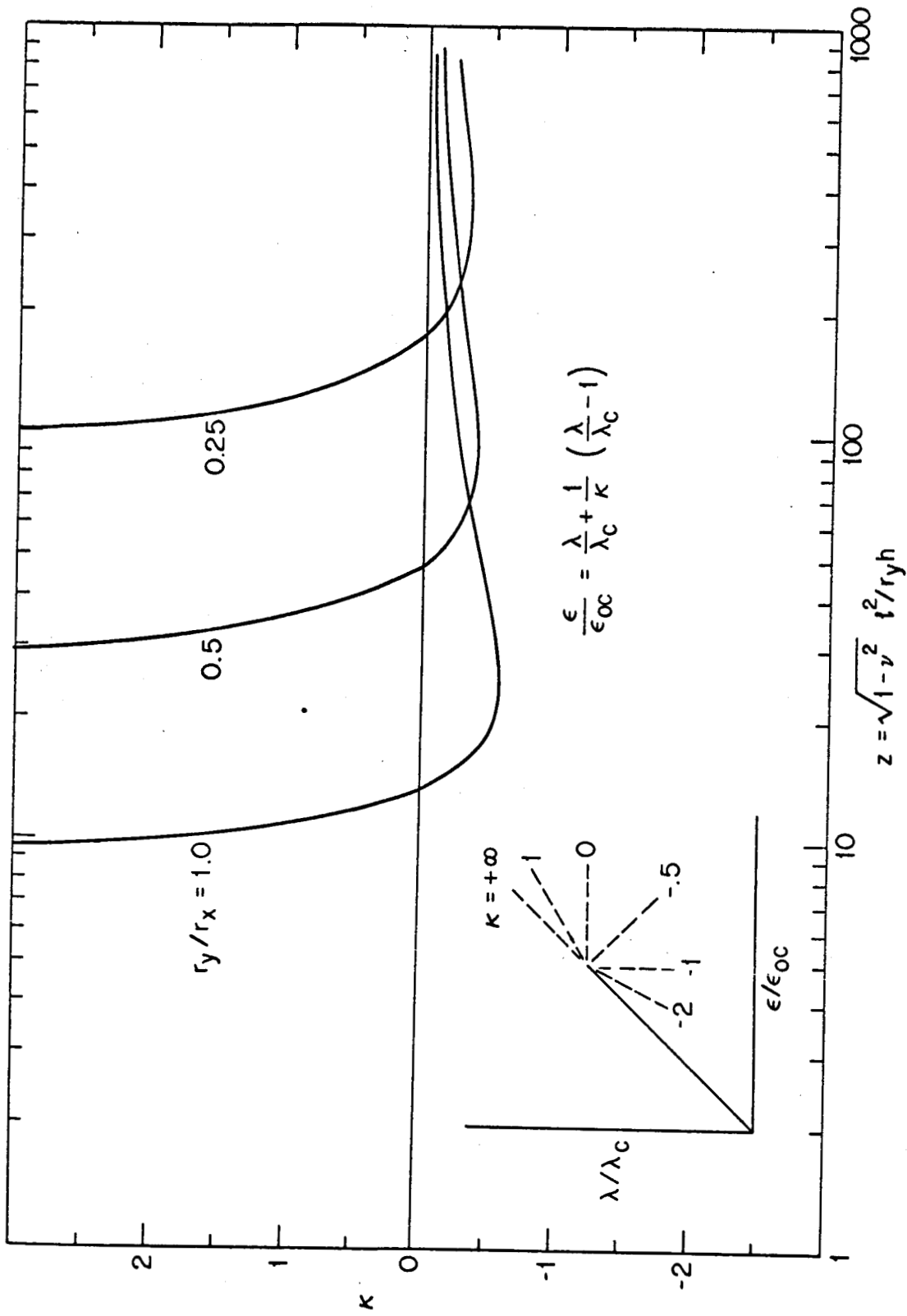


FIG. 11 LOAD-ELONGATION RELATION IN INITIAL POST-BUCKLING OF TOROIDAL SEGMENTS SUBJECT TO AXIAL TENSION [ $\nu = 1/3$ ]